**FLYWHEEL: JURNAL TEKNIK MESIN UNTIRTA**

Homepagejurnal: http://jurnal.untirta.ac.id/index.php/jwl

# Decay Curve Analysis of a Damped Vibration System with Multi-force Perturbations

A. Y. Ismail*, A. Noerpamoengkas, S. B. Sasongko

*Department of Mechanical Engineering, Institut Teknologi Adhi Tama Surabaya, 100th Arif Rachman Hakim St., Surabaya, 60165, Indonesia.*

*Corresponding author: *yusuf@itats.ac.id*

*ARTICLE INFO*

Received 04/09/2023
revision 13/11/2023
accepted 23/11/2023
Available online 05/12/2023

*ABSTRACT*

Perturbation in a system is one of the troublesome matters in dynamics, vibration, and control. It changes the system's behavior and possibly causes a mechanical failure. This paper presents the effect of perturbations on the decay curve of a damped vibration system. The perturbations are varied from single to multiple forces to give novel knowledge completing previous studies. Additionally, the system properties, i.e., damping and stiffness, are also varied to provide more meaningful comprehensive information and, thus, can be used in further vibrational system developments. The result shows that the multiplication of perturbation force significantly changes the decay curve slope with unique characteristics. The variation of damping and stiffness also affects the vibration amplitude and the system resonance.

**Keywords:** *vibration, damping, decay curve, multi-force, perturbation.*

## 1. INTRODUCTION

Investigating perturbations and their impact on vibration dynamics and control has garnered substantial attention [1–5]. This study delves into the relationship between perturbations and mechanical failure, aiming to unravel novel insights into this complex interplay. Vibration phenomena, including perturbations, play a pivotal role in various scientific domains, from molecular spectroscopy to mechanical engineering [6–12], where understanding oscillatory systems' intricate behavior is paramount [13].

For instance, Chang et al. [14], adopt the large-order Rayleigh–Schrödinger perturbation theory (RSPT) to compute vibrational states in linear molecules. Their work delves into applying this theory in the context of various molecules, including $CO_2$ and $C_2H_2$, employing both isomorphic Watson Hamiltonian and quartic force fields. This investigation reveals intricate details about the effects of perturbations on vibrational states, presenting mathematical tools such as quartic Padé–Hermite approximants that prove indispensable in understanding resonance effects and singular points of eigenvalues on the complex plane.

Ditler et al. [15] explore the realm of *vibrational circular dichroism* (VCD) spectra in natural products through the lens of nuclear velocity perturbation theory. Their approach involves a sophisticated interplay between Gaussian and plane waves within the CP2K (*the open-source electronic structure and molecular dynamics software package*) framework, enabling the simulation of VCD spectra. By delving into the influences of various density functionals and their implications on conformational analysis and VCD spectra, the authors shed light on the intricate relationship between molecular moieties and their VCD contributions.

In another vein, Wang et al. [16] delve into the realm of electromechanical dynamics and vibration suppression in high-speed macro–micromanipulators with structural flexibility. Their study intertwines the theoretical aspects of assumed mode methods and the Prandtl-Ishlinskii hysteresis model to derive an electromechanical

dynamics model. By introducing a robust control strategy incorporating perturbation H-infinity control and Kalman filtering, they strive to counteract hysteresis nonlinearity and mitigate microscopic vibrations, even in parameter perturbations. The study underscores the potential of this control strategy in enhancing manipulation stability, robustness, and accuracy.

A unique perspective has been introduced, harnessing the concept of perturbation effects to devise a novel predictive model for human discomfort arising from these intertwined stimuli. A psycho-physics experiment was meticulously devised to discern the perturbation effect caused by noise stimulus. The study involved twelve participants, each subjected to an array of noise and vibration combinations. The participants rated their discomfort relative to reference stimuli after exposure to each combination. The findings unveiled a predictive equation for discomfort caused by vibration [2].

In a distinct avenue, the study by Yang et al. [4] delves into the chaotic vibrations of infinite-dimensional dynamical systems governed by linear hyperbolic *partial differential equations* (PDEs) in three-dimensional space. This study contributes a rigorous mathematical theorem certifying the occurrence of chaos in such systems. The central focus is on advancing chaos in the context of 3D hyperbolic PDEs, with illustrative examples demonstrating the practical implications of the theoretical chaotic results.

Ni et al. [17] embark on a study concerning the vortex-induced vibration of a two-degree-of-freedom cylinder. The objective is to investigate the influence of perturbations on the bifurcation characteristics of vortex-induced vibration and offer engineering insights. The study observes variations in amplitude, frequency, lift, and drag coefficients of the cylinder's vibration response after perturbing its displacement. Through vorticity map analysis, the study reveals that displacement perturbations induce changes in the cylinder's motion state and influence the shedding and wake modes of the vortex. The study highlights the instability introduced by perturbations in the flow field and cylinder motion. Ultimately, the interaction between the perturbed flow field and cylinder motion stabilizes the upper or lower branch of bifurcation, contingent upon the perturbation's direction and magnitude. This study sheds light on the potential for the vortex-induced vibration of a cylinder to exhibit two relatively stable states near branch jump points, transformable under appropriate perturbations.

More researchers, besides those studies above, have also investigated vibration, particularly perturbation, in many other applications such as theoretical physics [18], chemical application [19], as well as structural engineering [20].

This paper eventually embarks on a fundamental exploration of the effects of multi-force perturbations on the damping characteristics of a common damped vibration system. Multi-force perturbations can be considered the frequent unpredictable factor in practical applications that causes major failures yet are rarely anticipated.

## 2. METHODOLOGY

### *2.1. Mathematical Model*

First, a mathematical model representing the common spring-mass system with excitation force is established for running transiently within $t$ = 0 – 10 seconds. Then, this system is added by the multi-force perturbation at $t$ = 4.5 seconds. The complete model is represented in Figure 1 below. It shows the system mass $m$, stiffness $k$, damping $c$, excitation force $fe$, and the perturbation force $fi$, whereas $i$ indicates the number of perturbations. The variation of the model is shown in the following sub-section.

The properties of the system are given as mass $m$ = 1 kg, damping loss factor $\xi$ = 0.05, and stiffness $k$ = 2500 N/m. The excitation force $fe$ is set to be 20 N and the perturbation force $fi$ is 50 N.

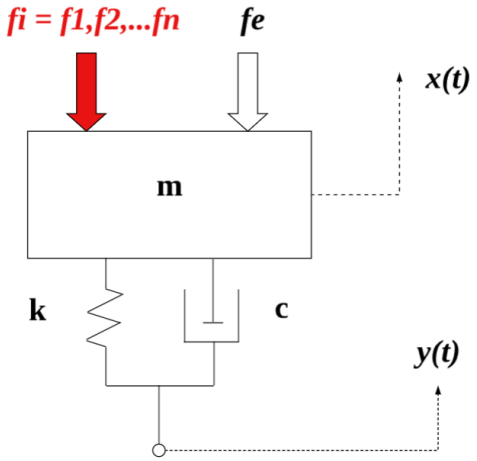


**Figure 1.** A single degree of freedom of damped vibration system with perturbations.

### *2.2. Parametric Study*

Table 1 shows the parametric study in this study. The perturbation varies from 1 up to 8 multiplications. The stiffness and damping coefficient are also varied to broaden the investigations.

**Table 1.** Parametric Study.

| Variable | Variation 1 | Variation 2 | Variation 3 | Variation 4 |
|---|---|---|---|---|
| Perturbation Force | $f_1 = f_i$ | $f_2 = 2f_i$ | $f_3 = 4f_i$ | $f_4 = 8f_i$ |
| Damping Coefficient | $\xi$ | $2\xi$ | $4\xi$ | $8\xi$ |
| Stiffness | $k$ | $2k$ | - | $4k$ |

## 3. RESULTS AND DISCUSSION

### *3.1. Governing Equation*

From the model in Figure, the equation of motion containing both excitation force as well as perturbation force can be written as:

$$m\ddot{x} + c\dot{x} + kx = c\dot{y} + ky - fe - fi \quad (1)$$

This paper's main area of interest is where *fe* is the excitation force and $fi = f1, f2, \ldots fn$ is the multi-perturbation force. Again, *i* indicates the number of perturbations. Moving the stiffness and damping elements on the same side gives:

$$m\ddot{x} + c(\dot{x} - \dot{y}) + k(x - y) = fe - fi \quad (2)$$

Then, the acceleration amplitude can be written by dividing all sides with mass *m* as:

$$\ddot{x} = \frac{c}{m}(\dot{x} - \dot{y}) + \frac{k}{m}(x - y) - \frac{fe}{m} - \frac{fi}{m} \quad (3)$$

From here, the displacement position can be obtained by integration. The integration is automatically generated using the ordinary differential equation (ODE) solver in the Python package. The code is developed by expanding the code by Vaughan [21].

Figure 2 shows the position of mass *m* within a 10-second oscillation. It can be seen that the excitation force acts at the 1st second and the damping effect up to 4 seconds. Then, the perturbation starts at 4.5 seconds indicated by the striking increment of the position amplitude up to 1.5 m. From there, the decay curve shown by the black dashed line can be observed.

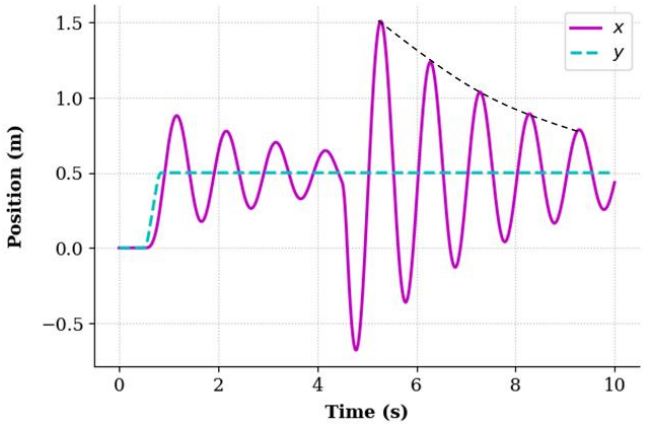


**Figure 2.** Analytical results of the model.

Figure 2 shows the position of mass *m* within a 10-second oscillation. It can be seen that the excitation force acts at the 1st second and the damping effect up to 4 seconds. Then, the perturbation starts at 4.5 seconds indicated by the striking increment of the position amplitude up to 1.5 m. From there, the decay curve shown by the black dashed line can be observed.

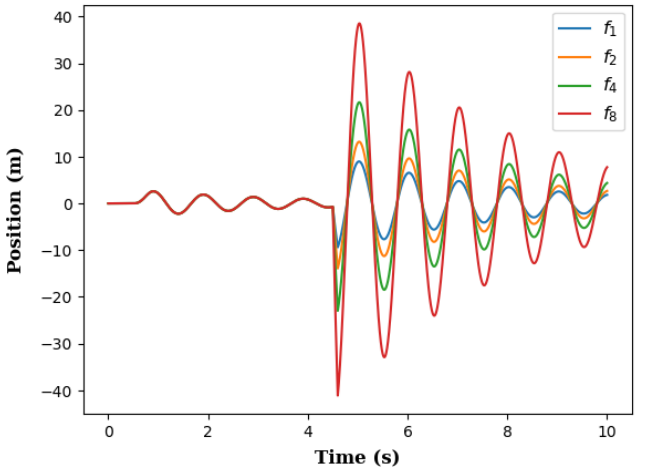


**Figure 3.** The variation of the number of perturbations.

From the figure also, we can see the steady position of y starts from the excitation force starts or 1st second until 10 seconds. This explains the assumption made in the introduction section that in practice, machines usually reach a steady condition after being initiated.

### *3.2. Parametric Study*

Figure 3 shows the effect of perturbations number from 1, 2, 4, until 8 forces, while the excitation force is kept constant. It is seen that the multiplications of the perturbation forces significantly increase the position amplitude of *m*, even up to 40 m. The amplitude increment can be observed as having a

linear pattern from 1 to 8 perturbations proportional to the ODE equation, where the linearity of the increment is typical in both peak and valley oscillations. This phenomenon also agrees with the harmonic oscillatory of a damped vibration system in [22].

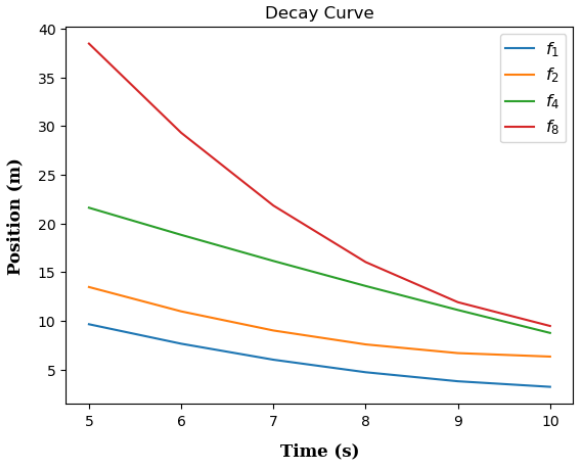


**Figure 4.** The effect of perturbation multiplication on the decay curve.

The decay curve is shown in Figure 4. In general, all variations have a common reasonable damping effect, as shown by the slope of the decay curve. The slope for the first perturbation force has a linear increment with the second one, which is obtained by doubling the perturbation. When the doubling continues, the slope shows a slight difference, as seen in the third slope. Significant slope differences occur at the last variations, whereas the perturbation is multiplied 8 times. The decay curve has the steepest slope and shows more non-linearity. This happens since the damping coefficient, which is kept constant, meets the sudden high perturbation forces.

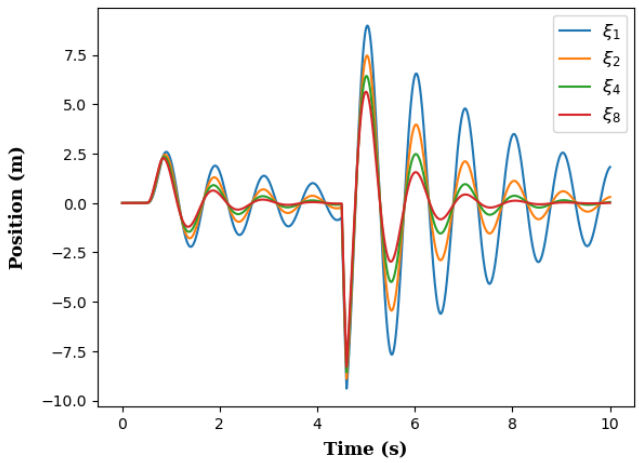


**Figure 5.** The variation of damping loss factor.

Figure 5 shows the variation of the damping loss factor in the spring-mass system. Since the damping is introduced in the system since the initiation, the effect occurs both before and after the perturbation force is actuated. The variation itself is also linearly gradual, resulting in linear damping as well. Again, this phenomenon is similar to the previous study [22]. It can be observed in the reduction of the position amplitude from around 7.5 m (the first amplitude of position after perturbation) to 5 m, the last damping loss factor variation. This decrement pattern is proportional if we see the second amplitude and upwards, where the amplitude has typical decrements.

The decay curve for the damping loss factor variation is shown in Figure 6, showing the amplitude reduction more clearly. The slope differences have the same pattern as the previous variation, whereby increasing the damping loss factor also reduces the decay curves significantly.

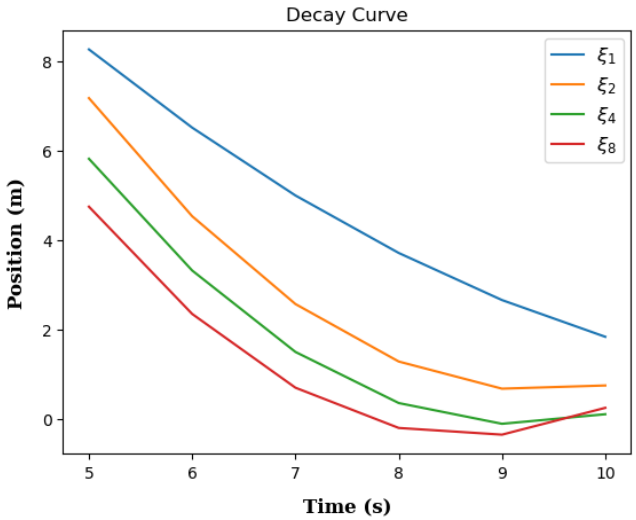


**Figure 6.** The effect of damping loss factor on the decay curve.

The variation of stiffness is shown in Figure 7. Unlike the previous two variations, the changes in stiffness not only change the position amplitude but also shift the overall oscillations forward. This is due to the change of *k/m* value in Eq (3), which represents the system's natural frequency. Natural frequency is known as a significant factor of a system that determines the system's resonance. A bit of change in the natural frequency will change the system behavior significantly. This is also explained by previous study [13]. Here, in Figure 7, the variation of *k* is proportional to the frequency changes indicated by the amplitude shifting and the number of oscillations. The increase of the *k* value results in the increment value of natural frequency *k/m*, which increases the oscillation numbers.

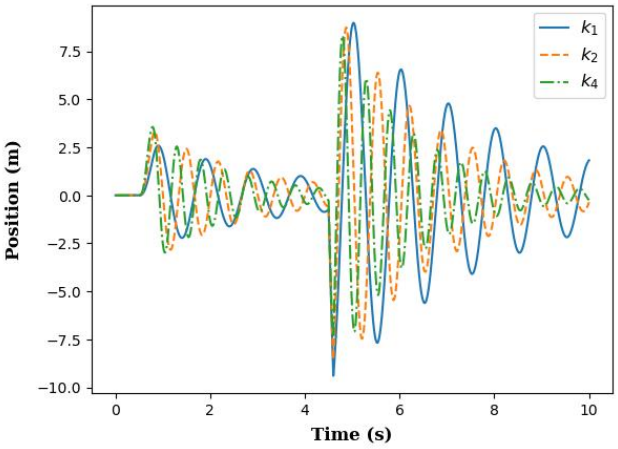


**Figure 7.** The variation of stiffness.

Meanwhile, the amplitude also shows some interesting findings to be explored. Before the perturbation starts, increasing the stiffness tends to increase the amplitude due to extra inertia. However, after the perturbation, this phenomenon flips into the opposite way. Increasing the stiffness instead reduces the amplitude. This happens because, at some points, the additional forces from perturbation reduce the inertia effect from adding stiffness. In other words, the increment perturbation forces give a more dominant effect than the inertia increment from the stiffness. Therefore, the amplitude after perturbation behaves oppositely to that before perturbation.

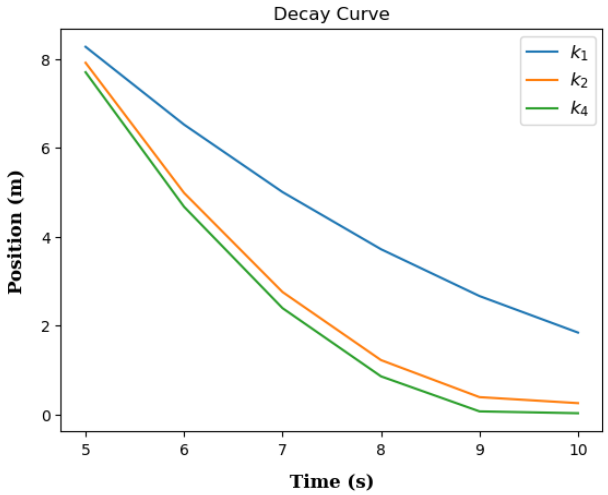


**Figure 8.** The effect of stiffness on the decay curve.

Otherwise, the decay curve for the variation is shown in Figure 8 below. Since the variation is only in three different values, the difference is seen in the Figure. In terms of slope, the increment of $k$ significantly increases the decay curve slope. This can be seen in the $k_1$ and $k_2$ curves. However, this phenomenon has a limited boundary since further increment from $k_2$ to $k_3$ only changes the curve amplitude without considerable changes in the slope. This needs further and deeper investigation.

## 4. CONCLUSION

An analytical study on the effect of multi-force perturbations on the decay curve has been presented. It is known that multiplying the perturbation force significantly increases the decay curve slope. It is also known that increasing the damping gives a linear or proportional reduction in the vibration amplitude with multi-force perturbations. Moreover, varying the system stiffness gives changes in the vibration amplitude and decay curve slope and shifts the oscillations forward due to changes in the natural frequency. This result could be further investigated by involving the concept of natural frequency in discussions.

## ACKNOWLEDGMENTS

The authors would like to thank the Laboratory of Vibration, Department of Mechanical Engineering ITATS, for supporting this research, including facilities and funding.

## REFERENCES

1. Kevrekidis PG. Multipulses in discrete Hamiltonian nonlinear systems. Phys Rev E - Stat Physics, Plasmas, Fluids, Relat Interdiscip Top. 2001;64(2):5.

2. Aladdin MF, Jalil NAA, Guan NY, Rezali KAM. Perturbation effect of noise on overall feeling of discomfort from vertical whole-body vibration in vibro-acoustic environment. Int J Ind Ergon. 2021;83(May):103136.

3. Sinha V, Ghorai PK. CO adsorption on FeN(N = 1-4) transition metal clusters: A density functional theory study. Curr Sci. 2014;106(9):1243–8.

4. Yang Q, Xiang Q. Chaotic vibrations of 3D linear hyperbolic PDEs with linear perturbations of superlinear boundary conditions. J Math Anal Appl. 2022;507(1):125743.

5. Chauhan S, Kumar M, Chhoker S, Katyal SC. A comparative study on structural, vibrational, dielectric and magnetic properties of microcrystalline BiFeO3, nanocrystalline BiFeO3and core-shell structured BiFeO3@SiO2nanoparticles. J Alloys Compd. 2016;666:454–67.

6. Zhao H, Ding Y, Li A, Chen B, Zhang X. State-monitoring for abnormal vibration of bridge cables focusing on non-stationary responses: From knowledge in phenomena to digital indicators. Meas J Int Meas Confed. 2022;205:112148.

7. Wu MQ, Zhang W, Niu Y. Experimental and numerical studies on nonlinear vibrations and dynamic snap-through phenomena of bistable asymmetric composite laminated shallow shell under center foundation excitation. Eur J Mech A/Solids. 2021;89:104303.

8. Gao T, Cao S. Paroxysmal impulse vibration phenomena and mechanism of a dual–rotor system with an outer raceway defect of the inter-shaft bearing. Mech Syst Signal Process. 2021;157:107730.

9. Hossein Rabiee A, Rafieian F, Mosavi A. Active vibration control of tandem square cylinders for three different phenomena: Vortex-induced vibration, galloping, and wake-induced vibration. Alexandria Eng J. 2022;61(12):12019–37.

10. Salvatore A. On the shock performance of a hysteretic tri-stable vibration isolation system: Nonlinear phenomena and optimization. Int J Non Linear Mech. 2023;157:104557.

11. Yan J, Zhao R, Wan M, Meng B. Coupled effect of pulsed current and ultrasonic vibration on deformation behavior of Inconel 718 sheet: phenomena and modeling. J Mater Res Technol. 2023;25:5538–60.

12. Rosso M, Kohtanen E, Corigliano A, Ardito R, Erturk A. Nonlinear phenomena in magnetic plucking of piezoelectric vibration energy harvesters. Sensors Actuators A Phys. 2023;362:114667.

13. Firman LOM, Dwi R, Budhi MS. The application of Vibration system on dryer machine to dry RDF and agricultural products by using Green Incinerator. Flywheel J Tek Mesin Untirta. 2019;V(1):83–9.

14. Chang X, Dobrolyubov EO, Krasnoshchekov S V. Vibrational resonance analysis of linear molecules using resummation of divergent Rayleigh–Schrödinger perturbation theory series. Spectrochim Acta - Part A Mol Biomol Spectrosc. 2023;288:122071.

15. Ditler E, Kumar C, Luber S. Vibrational circular dichroism spectra of natural products by means of the nuclear velocity perturbation theory. Spectrochim Acta - Part A Mol Biomol Spectrosc. 2023;298:122769.

16. Wang S, Yang Y ling, Li G ping, Du H lin, Wei Y ding. Microscopic vibration suppression for a high-speed macro-micro manipulator with parameter perturbation. Mech Syst Signal Process. 2022;179:109332.

17. Ni W, Zhang X, Xu F, Zhang W, Kang Z. Numerical investigation of bifurcation characteristics under perturbations in vortex induced vibration of cylinder with two degrees of freedom. Ocean Eng. 2019;188:106318.

18. Krasnoshchekov S V., Dobrolyubov EO, Chang X. Hypoflorous acid (HOF): A molecule with a rare (1,-2,-1) vibrational resonance and (8,3,2) polyad structure revealed by Padé-Hermite resummation of divergent Rayleigh-Schrödinger perturbation theory series. J Quant Spectrosc Radiat Transf. 2021;268:107620.

19. Pietropolli Charmet A, Bizzocchi L, Giuliano BM, Caselli P, Craig NC, Krasnoshchekov S V. Disentangling the IR spectra of 2,3,3,3-tetrafluoropropene using an ab initio description of vibrational polyads by means of canonical Van Vleck perturbation theory. J Quant Spectrosc Radiat Transf. 2019;239:106656.

20. Xu W, Zhu W, Su Z, Cao M, Xu H. A novel structural damage identification approach using damage-induced perturbation in longitudinal vibration. J Sound Vib. 2021;496:115932.

21. Vaughan J. MCHE485 Mechanical-Vibrations [Internet]. https://github.com. 2020. p. DocVaughan / MCHE485 – Mechanical – Vibrations. Available from: https://github.com/DocVaughan/MCHE485---Mechanical-Vibrations

22. Sudarmaji A, Putra AY, Yudiarsah E. Viscous damping coefficient measurement system using incremental optical encoder. Flywheel J Tek Mesin Untirta. 2023;9(1):1–7.